

Age-associated changes in intestinal fructose uptake are not explained by alterations in the abundance of GLUT5 or GLUT2

Laurie A. Drozdowski^a, Trudy D. Woudstra^a, Gary E. Wild^b, M. Tom Clandinin^a,
Alan B.R. Thomson^{a,*}

^a*Nutrition and Metabolism Group, Division of Gastroenterology, Department of Medicine, 5146 Dentistry Pharmacy Building, University of Alberta, Edmonton, AB T6G 2N8, Canada*

^b*Department of Anatomy and Cell Biology, McGill University, Montreal, PQ, Canada*

Abstract

A reduction in nutrient absorption may contribute to malnourishment in the elderly. The objectives of this study were to determine the effects of aging on the absorption of fructose in rats, as well as the mechanisms of these adaptive changes. Male Fischer 344 rats aged 1, 9, and 24 months were fed standard Purina chow for 2 weeks (PMI #5001, PMI Nutritionals, Brentwood, MO). The uptake of ¹⁴C-labeled D-fructose was determined in vitro using the intestinal sheet method. Intestinal samples were taken for RNA isolation and for brush border membrane (BBM) and basolateral membrane (BLM) preparation. Northern blotting, Western blotting, and immunohistochemistry were used to determine the effects of age and diet on GLUT5 and GLUT2. When expressed on the basis of intestinal or mucosal weights, aging was associated with a decline in jejunal and ileal fructose uptake, whereas jejunal fructose uptake was increased when expressed on the basis of serosal or mucosal surface area. The alterations in fructose uptake were not paralleled by changes in GLUT5 or GLUT2 abundance. These results indicate that 1) the effect of age on fructose uptake depends on the method used to express results, and 2) the age-associated changes in uptake are not explained by alterations in GLUT5 and GLUT2. © 2004 Elsevier Inc. All rights reserved.

Keywords: Aging; Fructose; Uptake; GLUT2; GLUT5

1. Introduction

The aging of the population has focused attention on the physiological processes associated with aging. Elderly individuals are at high risk for malnutrition. Although there are many physiological and social factors involved, a reduction in nutrient absorption may contribute to this malnourishment. A study using breath hydrogen analysis after a carbohydrate meal showed evidence of malabsorption in the elderly [1]. Similarly, transport experiments using isolated brush border membrane (BBM) vesicles demonstrated a reduction in Na⁺-dependent D-glucose uptake in older patients [2]. In contrast, a study by Wallis et al. did not find changes in Na⁺-dependent glucose transport in BBM vesicles isolated from human duodenal biopsy samples [3].

The results from experiments using rodent models of aging also demonstrate conflicting results. Several studies show reductions in D-glucose absorption in aged rats [4–6]. A normal

or increased absorptive capacity, depending on the site studied, was also found in a study using everted intestinal segments from old versus young rats [7]. Results from studies in mice also do not provide conclusive results on the effect of aging on nutrient absorption. Ferraris et al. show a reduction in uptake and site density of sodium-dependent glucose transporter in BBM in aged mice [8]. This is in contrast to the findings of Thompson et al., who showed an increase in intestinal glucose uptake in aged mice [9].

The discrepancies in the results from studies in humans, rats, and mice may be due to the differences in the methodologies that were used. Although some investigators have studied uptake using BBM vesicles [2–6], others have used everted intestinal rings [7–9]. The method of expressing results is also important. Most studies have expressed uptake based on intestinal weight and have therefore failed to take into account any potential age-associated changes in mucosal weight or surface area. The strain of the animals used, the ages of the animals, and the site of the intestine used may also differ among studies and may explain the variability in results.

* Corresponding author. Tel.: (780) 492-6490; fax: (780) 492-7964.
E-mail address: alan.thomson@ualberta.ca (A. Thomson).

The uptake of fructose has been studied in aging mice. Ferraris et al. showed that D-fructose uptake per milligram of tissue was higher in the jejunum of young animals than in older animals [8]. Adaptive increases in uptake, in response to increasing carbohydrate levels, were blunted in aged mice and were restricted to more proximal regions of the small intestine [10].

The uptake of fructose across the BBM is mediated by GLUT5, a sodium-independent facilitative transporter [11]. The transport of fructose and glucose out of the enterocyte across the basolateral membrane (BLM) occurs via the facilitative sodium-independent transporter of GLUT2, a sodium-independent glucose and fructose transporter [11]. In addition to its role as a BLM transporter, GLUT2 has now been localized in the BBM, where it has been suggested to contribute to the uptake of sugars into the enterocyte [12–15].

The objectives of this study were to determine 1) the effects of aging on the *in vitro* uptake of fructose in rats fed chow; and 2) the molecular mechanisms of these age-associated changes.

2. Methods and materials

2.1. Animals

The principles for the care and use of laboratory animals, approved by the Canadian Council on Animal Care and the Council of the American Physiological Society, were observed in the conduct of this study. A total of 18 male Fischer 344 rats aged 1, 9, and 24 months were obtained from the National Institute of Aging colony from Harlan Laboratories (Indianapolis, IN). Pairs of rats were housed at a temperature of 21°C, with 12 hours of light and 12 hours of darkness. Water and food were supplied *ad libitum*.

Animals were fed a standard PMI #5001 rodent chow diet. There were six animals in each of the three age groups. Animal weights were recorded at weekly intervals.

2.2. Uptake studies

2.2.1. Probe and marker compounds

The [¹⁴C]-labeled D-fructose was supplied by Amersham Biosciences Inc. (Baie D'Urfe, PQ, Canada) and the unlabeled fructose by Sigma Chemical (St. Louis, MO). The concentrations of fructose used were 8, 16, 32, and 64 mmol/L. [³H]-inulin was used as a nonabsorbable marker to correct for the adherent mucosal fluid volume.

2.2.2. Tissue preparation

The animals were sacrificed by an intraperitoneal injection of sodium pentobarbital (Euthanyl; 240 mg/100 g body weight). The whole length of the small intestine was then rapidly removed and rinsed with cold saline (Bimeda-MTC, Cambridge, Ontario, Canada). The intestine was opened

along its mesenteric border, and pieces of the proximal segment (jejunum) and distal segment (ileum) were cut and mounted as flat sheets in the transport chambers. A 5-cm piece of each jejunal and ileal segment of tissue was gently scraped with a glass slide to determine the percentage of the intestinal wall comprised of mucosa. The chambers were placed in preincubation beakers containing oxygenated Krebs-bicarbonate buffer (pH 7.2) at 37°C, and tissue discs were preincubated for 15 minutes to allow the tissue to equilibrate at this temperature. The rate of fructose uptake was determined from the timed transfer of the transport chambers to the incubation beakers containing [³H]-inulin and ¹⁴C-labeled fructose in oxygenated Krebs-bicarbonate (pH 7.2, 37°C). Preincubation and incubation chambers were mixed with circular magnetic bars at identical stirring rates, which were precisely adjusted using a strobe light. Stirring rates were reported as revolutions per minute (rpm). A stirring rate of 600 rpm was selected to achieve low effective resistance of the intestinal unstirred water layer [16–18].

2.2.3. Determination of uptake rates

After incubating the discs in labeled solutions for 6 minutes, the experiment was terminated by removing the chamber and rinsing the tissue in cold saline for approximately 5 seconds. The exposed mucosal tissue was then cut out of the chamber with a circular steel punch, placed on a glass slide, and dried overnight in an oven at 55°C. The dry weight of the tissue was determined, and the tissue was transferred to scintillation counting vials. The samples were saponified with 0.75 mol/L NaOH, scintillation fluid was added, and radioactivity was determined by means of an external standardization technique to correct for variable quenching of the two isotopes [16].

The rates of uptake of fructose were determined as $\text{nmol} \cdot 100 \text{ mg tissue}^{-1} \cdot \text{min}^{-1}$, $\text{nmol} \cdot 100 \text{ mg mucosal tissue}^{-1} \cdot \text{min}^{-1}$, and $\text{nmol} \cdot \text{cm}^{-2}$ serosal surface area min^{-1} , and $\text{nmol} \cdot \text{cm}^{-2}$ villus surface area min^{-1} . Because the relationship between uptake and fructose concentration was linear, the slopes of the lines were calculated and compared to determine statistical differences. Statistical significance was accepted for values with $P < 0.05$.

2.3. Morphology, mRNA, and protein analysis

2.3.1. Tissue preparation

An additional group of 12 animals (four in each of the three age groups) were raised and sacrificed similarly as for the uptake studies. A 5-cm portion of proximal jejunum and distal ileum was rinsed, quickly harvested, snap-frozen in liquid nitrogen, and stored at -80°C for subsequent mRNA isolation. Mucosal scrapings were harvested from the remaining proximal and distal small intestine, snap-frozen in liquid nitrogen, and stored at -80°C for later isolation of cellular components. For morphology and immunohisto-

chemistry analysis, two 1-cm pieces of proximal and distal small intestine were fixed in 10% formalin.

2.3.2. Morphological measurements

Morphometric data were obtained from hematoxylin and eosin-stained paraffin sections. Measurements were taken of villous height, villous width at one-half villous height, villous bottom width, and crypt depth. Horizontal cross sections were prepared so that villous thickness could be measured at one-half villous height. Magnification was calibrated using a micrometer. Mucosal surface area was calculated as previously described [19]. The number of villi per millimeter of serosal length was measured in longitudinal and horizontal cross sections, then multiplied together to obtain the number of villi per square millimeter serosa. When this villous density was multiplied by villous surface area, the result was the mucosal surface area, expressed as square millimeters per square millimeter of serosa. At least 10 villi were assessed per section. The following two formulae were used [19]: villous surface area ($\mu\text{m}^2/\text{villus}$) = $(2 \times M \times H) + (2 \times M - A) \times D + (2 \times D) \times [(A - M)^2 + (H)^2]^{0.5} \times 1000$, where H = villous height, M = villous width at one-half height, A = villous bottom width, and D = villous thickness. Mucosal surface area (mm^2/mm^2 serosa) was calculated as the number of villi/ mm^2 serosa \times villus surface area ($\mu\text{m}^2/\text{villus}$)/1000.

2.3.3. Abundance of mRNA

The intestinal pieces were homogenized in a denaturing solution containing guanidinium thiocyanate, using the Fast Prep cell disruptor (Savant Instruments, Holbrook, NY). After addition of 2 mol/L sodium acetate, a phenol chloroform extraction was performed. The upper aqueous phase containing the RNA was collected. RNA was precipitated with isopropanol overnight at -80°C , with a final wash with 70% ethanol. The concentration and purity of RNA was determined by spectrophotometry at 260 and 280 nm. Samples were stored at -80°C until use for Northern blotting, or for reverse transcriptase–polymerase chain reaction.

A 15- μg quantity of total RNA was fractionated by agarose gel electrophoresis and transferred to nylon membranes by capillary diffusion. RNA was fixed to the membranes by baking at 80°C for 2 hours. Northern blotting was performed using the DIG Easy Hyb method, according to the manufacturers protocol (Roche Diagnostics, Laval, PQ, Canada). The GLUT2 and GLUT5 plasmids were kindly donated by Dr. G.I. Bell of the Howard Hughes Medical Institute, University of Chicago.

The density of the mRNA bands was determined by transmittance densitometry (model GS-670 imaging densitometer; Biorad Laboratory, Mississauga, ON, Canada). Quantification of the 28 S ribosomal units from the membranes was used to account for loading discrepancies.

2.3.4. Protein analysis

We isolated BBM, BLM, and enterocyte cytosol rat intestinal mucosal scrapings by differential centrifugation and Ca^{2+} precipitation [20–22]. Aliquots were stored at -80°C .

The protein concentration of the samples was determined using the Bio-Rad Protein Assay (Life Science Group, Richmond, CA). Proteins were separated by sodium dodecyl sulfate-polyacrylamide gel electrophoresis and were transferred to nitrocellulose membranes by electroblotting.

Transfer efficiency was verified by staining of membranes with 3-hydroxy-4-(2-sulfo-4-[4-sulphophenylazo]-phenylazo)-2,7-naphthalenedisulfonic acid (Ponceau S) and by staining of gels with Coomassie Blue. Membranes were blocked by incubation overnight in Bovine Lacto Transfer Technique Optimizer (BLOTTO) containing 5% w/v dry milk in Tween Tris buffered saline (TTBS) (0.5% Tween 20, 30 mmol/L Tris, 150 mmol/L NaCl).

Membranes were washed in TTBS (3×10 minutes each) and were subsequently probed with specific rabbit antirat antibodies to GLUT5 (Chemicon International, Temecula, CA) and GLUT2 (Biogenesis, Poole, UK). Membranes were incubated for 2 hours at room temperature with the antibodies. Antibodies were diluted in 2% dry milk in TTBS at 1:500. Membranes were subsequently washed with TTBS to remove the residual unbound primary antibody, and were then incubated for 1 hour with goat anti-rabbit antibody (1:20000 in 2% dry milk in TTBS) conjugated with horseradish peroxidase (HRP) (Pierce, Rockford, IL).

Membranes were washed again in TTBS to remove residual secondary antibody, and were briefly incubated with Supersignal Chemiluminescent-HRP Substrate (Pierce, Rockford, IL). Membranes were exposed to X-OMAT AR films, and the relative band densities were determined by transmittance densitometry using Bio-Rad Imaging Densitometer (model GS-670 imaging densitometer; Biorad Laboratory, Mississauga, ON, Canada).

2.3.5. Immunohistochemistry

Jejunum and ileal tissue was embedded in paraffin. Sections 4–5 μm were then mounted on glass slides, dewaxed in xylene, and hydrated after incubation in a series of ethanol incubations. Slides were then incubated in hydrogen peroxide/methanol solution (20–50% H_2O_2 and 80% methanol) for 6 minutes, rinsed in tap water, and counterstained with Harris hematoxylin. Slides were then air-dried and the tissue was encircled with hydrophobic slide marker (PAP pen, BioGenex, San Ramon, CA). After rehydration in phosphate buffered saline, the slides were incubated for 15 minutes in blocking reagent (20% normal goat serum) followed by primary antibody to GLUT5 for 30 minutes. Slides were then washed in phosphate buffered saline and incubated in LINK and LABEL according to manufacturer protocol. The slides were subsequently incubated for 5 minutes in DAB solution (Biogenex, San Ramon, CA).

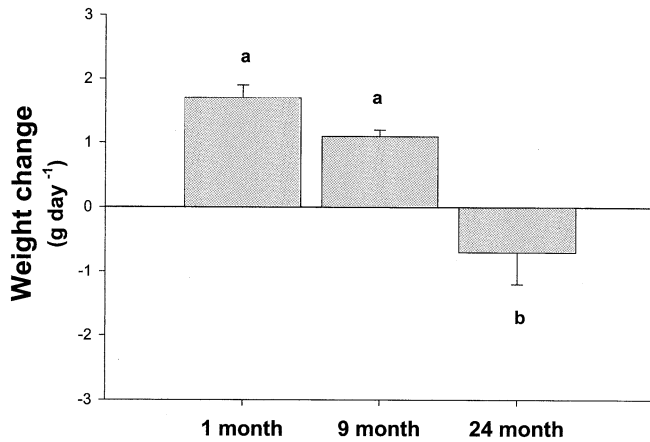


Fig. 1. Effect of age on body weight change in F344 rats. Values are mean \pm SEM. Different letters indicate a significant age effect (ANOVA, $P < 0.05$).

rinsed in water, dehydrated in absolute ethanol, and cleared in xylene. Negative controls were processed on the same slide in an identical manner, excluding the incubation with the primary antibody. A Leitz Orthoplan Universal Large-field microscope and a Leitz Vario Orthomat 2 automatic microscope camera were used to photograph the slides. Chromagen staining was quantified using a Pharmacia LKB-Imagemaster DTS densitometer and Pharmacia Imagemaster 1D, version 1.0, software (Amersham Pharmacia Biotechnology, Piscataway, NJ). Four villi per animal were quantified, and the results were normalized to the negative control values.

2.4. Statistical analysis

Results were expressed as mean \pm SEM. The statistical significance of the differences between the three age groups was determined by analysis of variance (ANOVA) ($P < 0.05$). Individual differences between ages were determined using a Student-Neuman-Keuls multiple range test. The Sigmatat version 1 statistical program was used for all statistical analysis.

3. Results

3.1. Animal characteristics

The rate of body weight change (g/day) was significantly lower at 24 months when compared to that of 1-month or 9-month-old animals (Fig. 1). Food intake was not influenced by the age of the rats (data not shown). Age did not affect the weight of the jejunum, the weight of the scraped jejunal mucosa, or the percentage of the jejunal wall comprised of mucosa (Table 1). In contrast, the weight of the ileum and the weight of the scraped ileal mucosa were

Table 1
Effect of age on intestinal weight

	1 Month	9 Months	24 Months
Tissue weight (mg/cm)			
Jejunum	9.0 \pm 0.7	12.3 \pm 1.3	10.7 \pm 1.5
Ileum	6.4 \pm 0.7 ^a	7.8 \pm 0.8 ^{ab}	11.1 \pm 1.7 ^b
Mucosal weight (mg/cm)			
Jejunum	4.0 \pm 0.5	6.3 \pm 1.2	5.6 \pm 1.1
Ileum	2.9 \pm 0.6 ^a	3.5 \pm 0.6 ^a	6.0 \pm 1.1 ^b
% of Mucosa			
Jejunum	44.5 \pm 2.9	48.8 \pm 5.2	48.7 \pm 4.0
Ileum	38.3 \pm 4.7	43.9 \pm 3.1	50.1 \pm 6.4

Values are mean \pm SEM.

Different superscript letters indicate a statistically significant age effect ($P < 0.05$).

approximately twice as high in animals 24 months old when compared to those of animals 1 month old.

There were no differences in the mean values of the heights of the villi of the jejunum or ileum of rats aged 1, 9, or 24 months (data not shown). Similarly, there were no differences in the jejunal or the ileal mucosal surface area at 1, 9, or 24 months (data not shown).

3.2. Fructose absorption

When fructose uptake was expressed on the basis of the weight of the entire wall of the intestine ($\text{nmol} \cdot 100 \text{ mg tissue}^{-1} \cdot \text{min}^{-1}$), there was reduced jejunal fructose uptake between 1 and 9 months but not between 1 and 24 months, whereas the ileal uptake of fructose was reduced at both 9 and 24 months (Fig. 2). When the rate of uptake was expressed on the basis of the weight of the mucosa ($\text{nmol} \cdot 100 \text{ mg mucosal tissue}^{-1} \cdot \text{min}^{-1}$), fructose uptake into the jejunum was lower at 9 and 24 months as compared to 1 month, and uptake into the ileum was lower at 9 months, but not at 24 months as compared to 1 month (Fig. 3). When uptake was expressed on the basis of serosal surface area, fructose uptake in the jejunum was higher at 24 than at 9 months or at 1 month and was unchanged by age in the ileum (Fig. 4). When uptake was expressed on the basis of mucosal surface area, jejunal fructose uptake was higher at 24 than at 9 months or 1 month, whereas ileal uptake was unaffected by age (Fig. 5). When the slopes of fructose uptake were compared, (Systat Software Inc., Point Richmond, CA) a significant decrease was seen at 9 and 24 months when compared to 1 month in both the jejunum and the ileum (Table 2).

3.3. Transporter protein abundance and immunohistochemistry

The jejunal abundance of GLUT5 in the BBM, as determined by Western blotting, was higher at 24 months as compared with 1 month (Fig. 6). The BBM abundance of GLUT5 in the ileum was similar at 1, 9, and 24 months. For

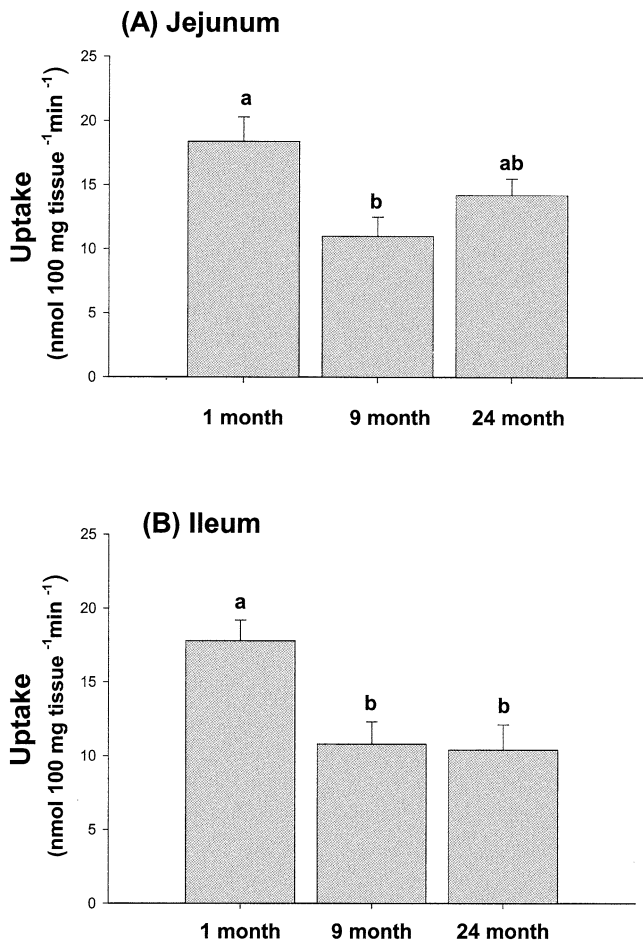


Fig. 2. Uptake of D-fructose expressed on the basis of intestinal weight in F344 rats. Values are mean \pm SEM of the slope of the linear regression as calculated using SigmaPlot (Systat Software, Inc, Point Richmond, CA). Different letters indicate a significant age effect (ANOVA, $P < 0.05$).

immunohistochemistry, jejunal and ileal villi were divided into five equal sections starting from the tip of the villi down to the crypt region. The abundance of GLUT5 protein was evenly distributed along the crypt–villus axis (Fig. 7). The jejunal abundance of GLUT5 was increased with aging (Fig. 8). In the ileum, GLUT5 was also increased at both 9 and 24 months as compared to that in animals 1 month of age.

The abundance of GLUT2 in the BLM was similar in 1-, 9-, and 24-month-old animals (data not shown).

3.4. Transporter mRNA abundance

The mRNA abundance of GLUT2 mRNA in the jejunum was similar in 1-, 9-, and 24-month-old animals (data not shown).

4. Discussion

The simplest way of expressing the rate of *in vitro* uptake of nutrients is on the basis of the weight of the full thickness

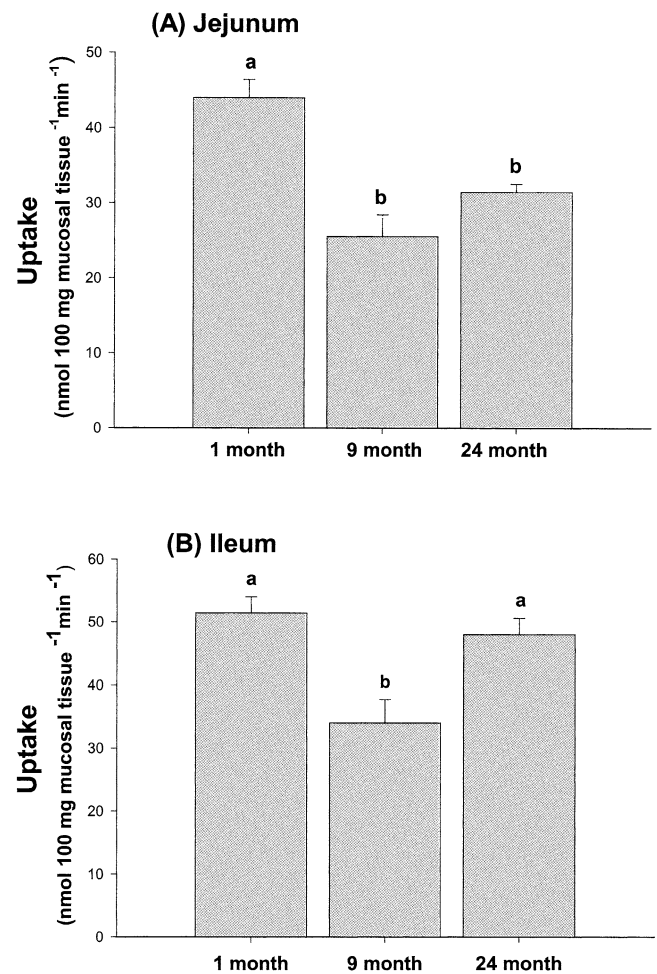


Fig. 3. Uptake of D-fructose expressed on the basis of mucosal weight in F344 rats. Values are mean \pm SEM of the slope of the linear regression as calculated using SigmaPlot. Different letters indicate a significant age effect (ANOVA, $P < 0.05$).

of the wall of the intestine. However, if a treatment alters the weight of the intestine, there may be variations in the rate of nutrient uptake that are understandable in light of there simply being more mucosal tissue. This may be an appropriate method of expressing the results of the uptake data when attempting to answer the question as to whether aging affects fructose absorption, but does not provide an explanation of the mechanisms of the age-associated alterations. For this reason, where there are treatment-associated variations in mucosal mass or the surface area of the villous membrane, then it is more appropriate to express uptake on the basis of mass of the transporting mucosal tissue or the mucosal surface area. When this was taken into consideration, aging was associated with a reduction in fructose uptake when expressed as intestinal or mucosal weight (Figs. 2 and 3), whereas aging was associated with increased jejunal fructose uptake when expressed as serosal or mucosal surface area (Figs. 4 and 5). Thus, the direction of the effect of aging on fructose uptake depends on the method used to express the rates of uptake.

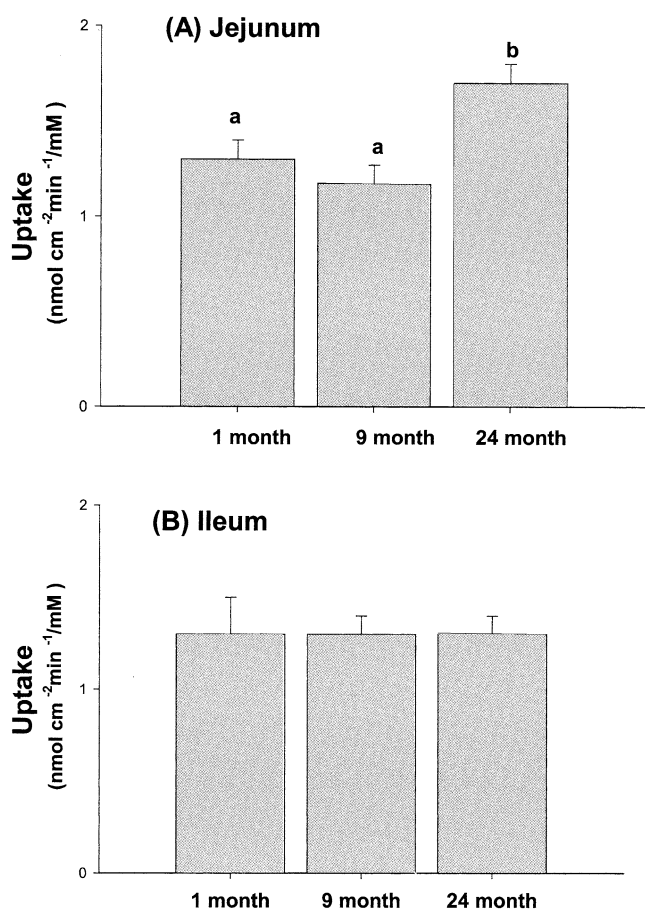


Fig. 4. Uptake of D-fructose expressed on the basis of serosal surface area in F344 rats. Values are mean \pm SEM of the slope of the linear regression as calculated using SigmaPlot. Different letters indicate a significant age effect (ANOVA, $P < 0.05$).

The changes in fructose uptake seen with aging are not explained by alterations in mRNA and protein abundance of the fructose transporters. At 24 months of age, the increase in jejunal fructose uptake expressed as serosal or mucosal surface (Figs. 4 and 5) is paralleled by increases in the abundance of GLUT5, as determined by Western blotting and by immunohistochemistry (Figs. 6 and 8). However, this does not apply when fructose uptake is expressed on the basis of intestinal or mucosal weight. In the ileum, between 1 month and 24 months of age, fructose uptake either falls (Fig. 2) or is unchanged (Figs. 3–5) depending upon how the data are expressed, and yet GLUT5 abundance is unchanged (Fig. 6) or increases (Fig. 8). Thus, the age-associated changes in the uptake of fructose is either associated with no change or an increase in the abundance of GLUT5 in the BBM.

In models of diabetes, a “recruitment” of transporters in the lower part of the villi results in active transport occurring in this area, and a resultant increase in glucose transport [23]. Changes in the distribution of GLUT5 along the crypt–villus axis might also explain changes in glucose uptake with aging. As most intestinal uptake occurs in the upper

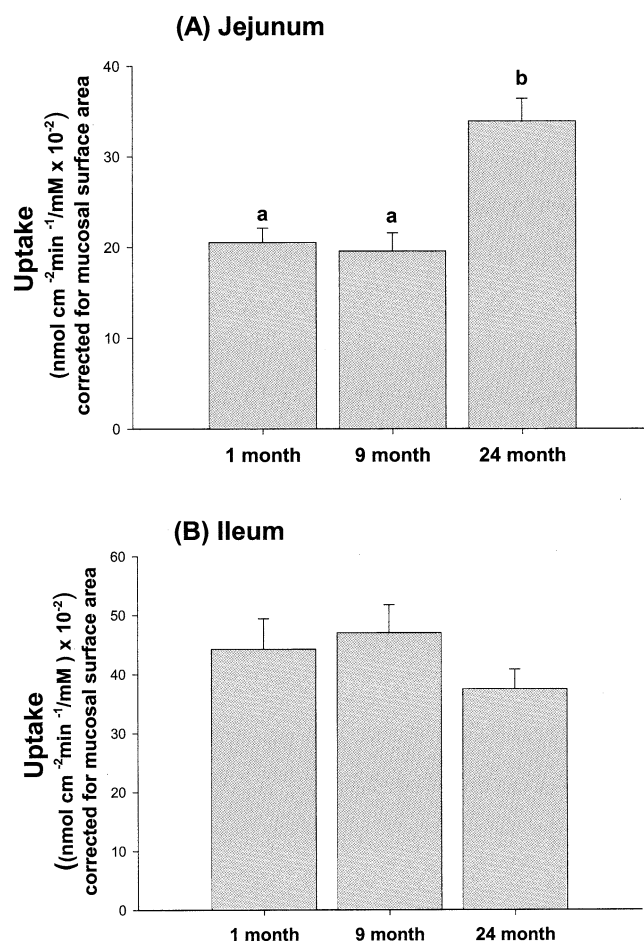


Fig. 5. Uptake of D-fructose expressed on the basis of mucosal surface area in F344 rats. Values are mean \pm SEM of the slope of the linear regression as calculated using SigmaPlot. Different letters indicate a significant age effect (ANOVA, $P < 0.05$).

third of the villi [24], a redistribution of transporter protein to this area may explain altered uptake. The results from this study do not show changes in the distribution of GLUT5 with age (data not shown), and thus it is unlikely that the age-associated changes in fructose uptake are due to the premature activation of transporters along the crypt–villus axis.

Table 2
Slopes for D-fructose uptake in the jejunum and ileum of Fischer 344 rats

Site	Age	Slope
Jejunum	1mo	44.4 \pm 2.4 ^a
	9mo	25.5 \pm 3.0 ^b
	24mo	31.4 \pm 1.1 ^b
Ileum	1mo	51.4 \pm 2.7 ^a
	9mo	26.8 \pm 4.0 ^b
	24mo	19.5 \pm 0.9 ^b

Data are mean \pm SEM.

Different superscript letters indicate a statistically significant age effect ($P < 0.05$).

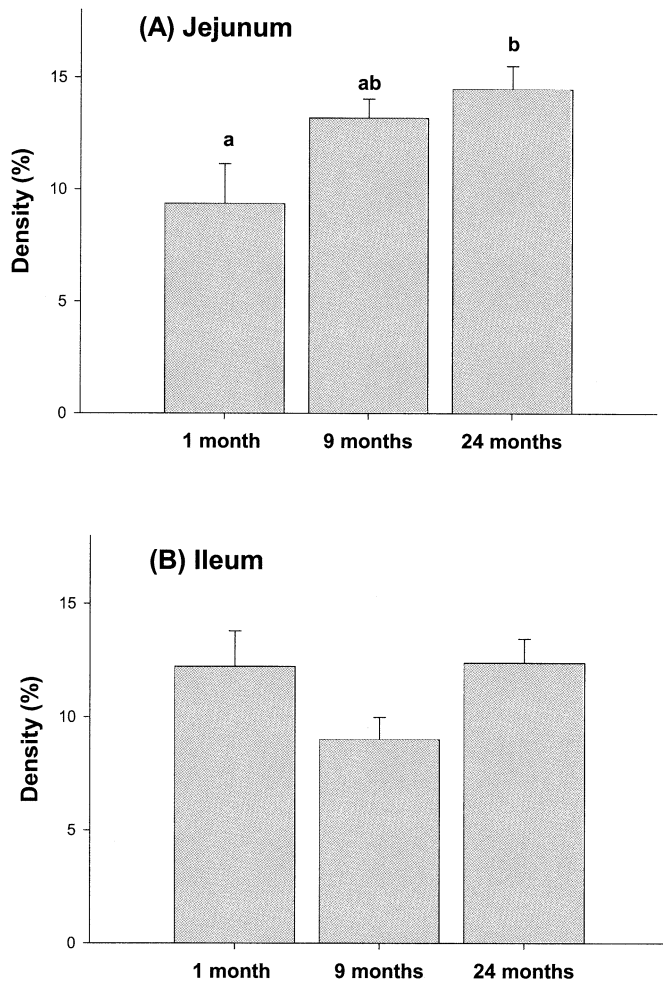


Fig. 6. Effect of age on GLUT5 protein abundance in F344 rats as determined by Western blotting. Values are mean \pm SEM. Different letters indicate a significant age effect (ANOVA, $P < 0.05$).

Changes in the fluidity of the BBM as a result of aging could also explain the apparent uncoupling of transport to gene abundance and protein abundance. There are reductions in the membrane fluidity of the BBM isolated from 117-week-old Fischer 344 rats as compared to younger animals [25]. Similarly, the fluorescence polarization technique used by Wahnou et al. showed reductions in membrane fluidity in 19-month-old rats when compared to 1- and 9-month-old rats [26]. Indeed, a study in chickens demonstrated that changes in BBM lipid content and fluidity may be involved in the alterations observed in D-glucose uptake during post-hatching development [27]. Although it is reasonable to speculate that the fluidity of the BBM may have fallen with aging, declines in membrane fluidity are associated with increases in uptake [28] rather than the variable results seen in this study.

It has been proposed that GLUT2 is present in the BBM as well as in the BLM [12–15] and transports glucose and fructose into the cell via facilitated diffusion. The changes in fructose uptake with aging may therefore be paralleled by

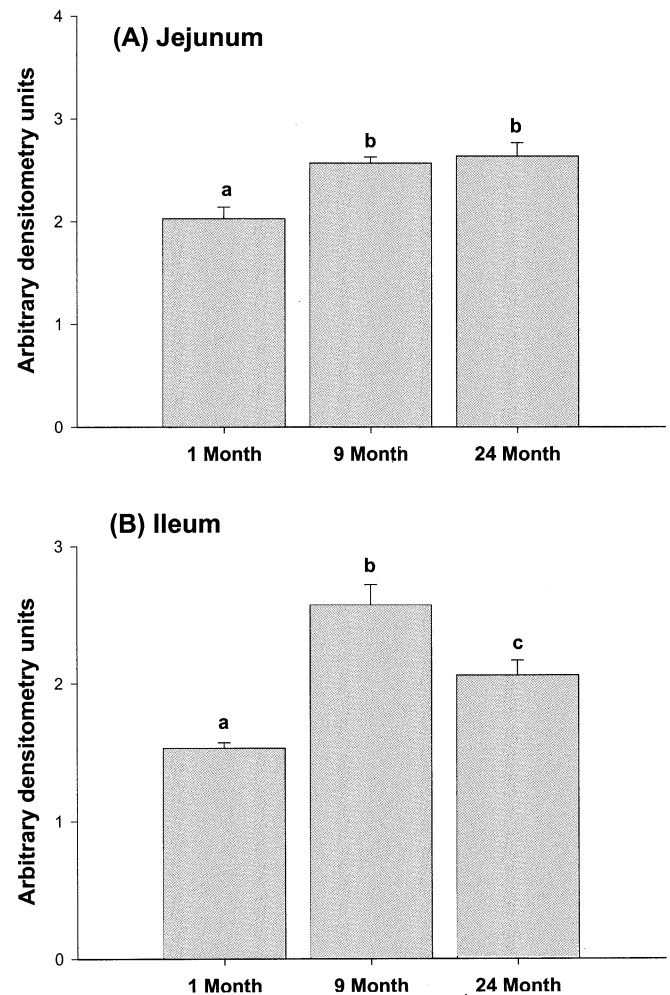


Fig. 7. Effect of age on GLUT5 abundance in F344 rats as determined by immunohistochemistry. Values are mean \pm SEM. Different letters indicate a significant age effect (ANOVA, $P < 0.05$).

alterations in BBM GLUT2 protein. This speculation cannot be confirmed in this study, as we do not have data for BBM GLUT2 protein abundance.

Other investigators have demonstrated that GLUT2 may not be essential for sugar absorption. In GLUT2-deficient mice (RIPGLUT1xGLUT2^{-/-}), an oral glucose load still resulted in a normal rate of glucose appearance in blood, suggesting that GLUT2 is not required [29]. Similarly, Stumpel et al. demonstrated identical kinetics of transepithelial glucose transport in GLUT2 deficient mice, when compared to control mice after oral glucose tolerance tests [30].

In summary, the results indicate that the effect of age on fructose uptake depends on the method used to express results. Although it may appear that fructose uptake is reduced with age, when reductions in mucosal surface area are taken into account, fructose uptake increases (as in the jejunum) or is unchanged (as in the ileum) with age. Finally, the age-associated changes in uptake are not fully explained by alterations in GLUT5 and GLUT2.

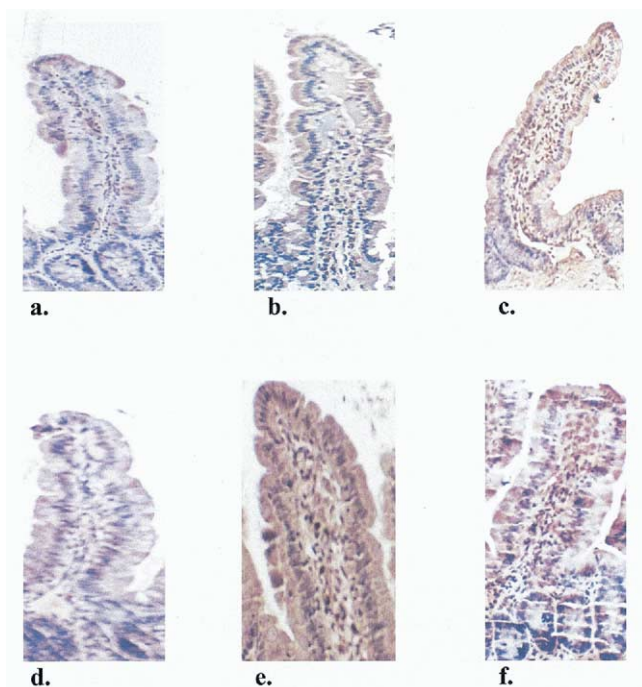


Fig. 8. GLUT5 immunohistochemistry on jejunal sections from F344 rats at ages (a) 1 month, (b) 9 months, and (c) 24 months; and on ileal sections from rats at ages (d) 1 month; (e) 9 months; and (f) 24 months.

Acknowledgments

We would like to acknowledge Elizabeth Wierzbicki and Terri Canuel for their technical assistance and Dr. Monika Keelan for her invaluable advice regarding the uptake calculations. We also acknowledge, with thanks, the contributions of Arnaud Brulaire, Stephanie Gabet and Marion Garel. Dr. Gary Wild is a senior clinician scientist supported by the Fonds de la Recherche en Santé du Québec.

References

- [1] Feibusch JM, Holt PR. Impaired absorptive capacity for carbohydrate in the aging human. *Dig Dis Sci* 1982;27:1095–100.
- [2] Vincenzini MT, Iantomasi T, Stio M, Favilli F, Vanni P, Tonelli F, Treves C. Glucose transport during ageing by human intestinal brush-border membrane vesicles. *Mech Ageing Dev* 1989;48:33–41.
- [3] Wallis JL, Lipski PS, Mathers JC, James OFW, Hirst BH. Duodenal brush-border mucosal glucose transport and enzyme activities in aging man and effect of bacterial contamination of the small intestine. *Dig Dis Sci* 1993;38:403–9.
- [4] Lindi C, Marciari P, Faelli A, Esposito G. Intestinal sugar transport during ageing. *Biochim Biophys Acta* 1985;816:411–4.
- [5] Freeman HJ, Quamme GA. Age-related changes in sodium-dependent glucose transport in rat small intestine. *Am J Physiol* 1986;251:G208–17.
- [6] Doubek WG, Armbrrecht HJ. Changes in intestinal glucose transport over the lifespan of the rat. *Mech Ageing Dev* 1987;39:91–102.
- [7] Darmenton P, Raul F, Doffoel M, Wessely JY. Age influence on sucrose hydrolysis and on monosaccharide absorption along the small intestine of rat. *Mech Ageing Dev* 1989;50:49–55.
- [8] Ferraris RP, Hsiao J, Hernandez R, Hirayama B. Site density of mouse intestinal glucose transporters declines with age. *Am J Physiol* 1993; 264:G285–93.
- [9] Thompson JS, Crouse DA, Mann SL, Saxena SK, Sharp JG. Intestinal glucose uptake is increased in aged mice. *Mech Ageing Dev* 1988;46:135–43.
- [10] Ferraris RP, Vinnakota RR. Regulation of intestinal nutrient transport is impaired in aged mice. *J Nutr* 1993;123:502–11.
- [11] Thorens B. Glucose transporters in the regulation of intestinal, renal, and liver glucose fluxes [Review]. *Am J Physiol* 1996;270:G541–53.
- [12] Kellett GL, Helliwell PA. The diffusive component of intestinal glucose absorption is mediated by the glucose-induced recruitment of GLUT2 to the brush-border membrane. *Biochem J* 2000;350:155–62.
- [13] Helliwell PA, Richardson M, Affleck J, Kellett GL. Stimulation of fructose transport across the intestinal brush-border membrane by PMA is mediated by GLUT2 and dynamically regulated by protein kinase C. *Biochem J* 2000;350:149–54.
- [14] Helliwell PA, Richardson M, Affleck J, Kellett GL. Regulation of GLUT5, GLUT2 and intestinal brush-border fructose absorption by the extracellular signal-regulated kinase, p38 mitogen-activated kinase and phosphatidylinositol 3-kinase intracellular signaling pathways: implications for adaptation to diabetes. *Biochem J* 2000;350:163–9.
- [15] Kellett G. The facilitated component of intestinal glucose absorption. *J Physiol* 2000;531:585–95.
- [16] Lukie BE, Westergaard H, Dietschy JM. Validation of a chamber that allows measurement of both tissue uptake rates and unstirred layer thicknesses in the intestine under conditions of controlled stirring. *Gastroenterology* 1974;67:652–61.
- [17] Westergaard H, Dietschy JM. Delineation of the dimensions and permeability of the two major diffusion barriers to passive mucosal uptake in the rabbit intestine. *J Clin Invest* 1974;54:718–32.
- [18] Westergaard H, Dietschy JM. The mechanism whereby bile acid micelles increase the rate of fatty acid and cholesterol uptake in the intestinal mucosal cell. *J Clin Invest* 1976;58:97–108.
- [19] Thomson ABR, McIntyre Y, McLeod J, Keelan M. Dietary fat content influences uptake of hexoses and lipids into rabbit jejunum following ileal resection. *Digestion* 1986;35:78–88.
- [20] Maenz DD, Cheeseman CI. Effect of hyperglycemia on D-glucose transport across the intestine. *Biochim Biophys Acta* 1986;860:277–85.
- [21] Orsenigo MN, Tosco M, Espisito G, Faella A. The basolateral membrane of rat enterocyte: its purification from brush border contamination. *Anal Biochem* 1985;144:577–83.
- [22] Orsenigo MN, Tosco M, Espisito G, Faelli A. Sodium transport in basolateral membrane vesicles from rat enterocytes. *Arch Int Physiol Biochim* 1987;95:57–66.
- [23] Burant CF, Flink S, DePaoli AM, Chen J, Lee W, Hediger MA, Buse JB, Chang EB. Small intestinal hexose transport in experimental diabetes. *J Clin Invest* 1985;93:578–85.
- [24] Thomson ABR, Cheeseman CI, Keelan M, Fedorak R, Clandinin MT. Crypt cell production rate, enterocyte turnover time and appearance of transport along the jejunal villus of the rat. *Biochim Biophys Acta* 1994;1191:197–204.
- [25] Brasitus TA, Yeh KY, Holt PR, Schachter D. Lipid fluidity and composition of intestinal microvillus membranes isolated from rats of different ages. *Biochim Biophys Acta* 1984;778:341–8.
- [26] Wahnou R, Mokady S, Cogan U. Age and membrane fluidity. *Mech Ageing Dev* 1989;50:249–55.
- [27] Vazquez CM, Rovira N, Ruiz-Gutierrez V, Planas JM. Developmental changes in glucose transport, lipid composition, and fluidity of jejunal BBM. *Am J Physiol* 1997;273:R1086–93.
- [28] Meddings JB, DeSouza D, Goel D, Thiesen S. Glucose transport and microvillus membrane physical properties along the crypt-villus axis of the rabbit. *J Clin Invest* 1990;85:1099–1107.
- [29] Thorens B, Guillam M-T, Beermann F, Burcelin R, Jaquet M. Transgenic reexpression of GLUT1 or GLUT2 in pancreatic beta cells rescues GLUT2-null mice from early death and restores normal glucose-stimulated insulin secretion. *J Biol Chem* 2000;275:23751–8.
- [30] Stumpel F, Burcellin R, Jungermann K, Thorens B. Normal kinetics of intestinal glucose absorption in the absence of GLUT2: evidence for a transport pathway requiring glucose phosphorylation and transfer into the endoplasmic reticulum. *Proc Natl Acad Sci USA* 2001;98:11330–5.